

Hydraulics of Roughness Mild Slope With Stacked Boulders in Half Trapezoidal Section

Youichi Yasuda, and Nozomi Fuchino

Department of Civil Engineering, College of Science and Technology, Nihon University, Tokyo, Japan

Abstract: Many kinds of fish passages have been installed in order to help the upstream migration for swimming fishes at hydraulic drop structures. Especially, pool-type fish passage was applied for both rest and upstream migration. In each pool, a plunging flow is formed, and also the capacity of discharge is limited in order to keep steady flow condition. For the formation of plunging flow, it is difficult for multi-aquatic animals to find the migration route. In this paper, roughness mild slope with stacked boulders in half trapezoidal section was presented as a new construction of fish passage. In proto type, around 50 cm long size was utilized as the stacked boulder. The longitudinal slope was settled as 1/25, and the fish passage had 4 m width with around 1/8 transverse slope. The migration route for multi-aquatic animals can be kept, even if the discharge changes from 0.45 m³/s to 3.2 m³/s. As the main flow passing over the roughness slope is always located near the water surface for several tailwater elevations, it might be easy to find the migration route.

Key words: stacked boulders, roughness mild slope, surface jet flow, diverse flow, migration route

1. Introduction

Fish passage has been installed at drop structure in order that swimming fishes can migrate upstream [1]. There are many kinds of fish passages [2]. Especially, pool-type fish passage has been applied for both rest and upstream migration. As the width of the fish passage is limited (e.g., 1.5 m to 4 m), the capacity for the change of discharge is limited in order to keep the steady flow condition [1, 3].

The author proposed the pool-type fish passage with trapezoidal section for the migration of multi-aquatic animals [4, 5]. In this case, the migration route is mainly near the water side. The formation of plunging flow at the downstream end of the fish passage does not lead aquatic animals to the fish passage. Many aquatic animals could not find the migration route of fish passage at the downstream of the drop structure [1, 2].

The roughness mild slope with stacked boulders is proposed as a new construction of the fish passage in this paper. The fish passage has 1/25 longitudinal slope, around 1/8 transverse slope, and 4 m width. The long size of stacked boulders was settled as around 50 cm in order to form a gap flow near the water side. The capacity for the change of discharges can be extended from 0.45 to 3.2 m³/s. In the case of the installation of the fish passage at tide weir, as a surface jet flow is always formed at the downstream of the fish passage, the concentration adjustment for diadromous aquatic animals between fresh water and sea water is possible for several tailwater elevations and discharges.

2. Experiments on Proposed Fish Passage

The experiments are conducted in a rectangular channel 17 m long, 0.4 m wide, 0.6 m high, at the Environmental Hydraulics Laboratory of Nihon University. As shown in Table 1, five different experiments are performed on the basis of Froude

Table 1 Experimental conditions in proto type.

Case	I_d (-)	I_{i1} (-)	I_{i2} (-)	I_{i3} (-)	Q_p (m ³ /s)	$T.L._p$ (m)
1	1/25	1/7	1/10	1/9	0.451	0.80, 1.09, 1.44
2	1/25	1/7	1/10	1/9	1.88	1.15, 1.37, 1.64, 1.87
3	1/25	1/7	1/10	1/9	3.25	1.32, 1.54, 1.75, 2.02
4	1/25	1/7	1/10	1/9	0.986	1.24, 1.61, 1.84
5	1/25	1/7	1/10	1/9	12.15	2.26

Here, I_d = longitudinal slope, I_{ii} = transverse slope in region i ($i = 1, 2, 3$), $T.L.$ = Tailwater Level, p = proto type.

similarity. Here, 1/10 scale model was applied. Five different discharges were studied. $Q_p = 12.15 \text{ m}^3/\text{s}$ in proto type was settled for a flood stage. For normal

stages (Cases 1 to 4), the effect of tailwater elevation on the formation of oriented flow at the downstream of the fish passage was examined. Photo 1 shows the installation of the roughness mild slope with the stacked boulders. In the experiments, the boulders were stacked without fixing with concrete etc. The averaged long size of the boulder is 0.05 m. As shown in Photo 2, the stepped channel with end sill was constructed in order to install the boulders easily by considering construction method. Longitudinal stepped channel has horizontal length 0.25 m and vertical height 0.01 m. Also, end sill has 0.01 m height in order to stack the boulder easily.



Photo 1 Roughness slope with stacked boulders in half trapezoidal section with 1/25 longitudinal slope. Physical model with 1/10 scale was installed in rectangular channel with 0.40 m width.



Photo 2 Stepped channel with end sill (transverse slope: $I_{i1} = 1/7$, $I_{i2} = 1/10$, $I_{i3} = 1/9$, $I_{i4} = 0$ from left to right). Transverse step: 0.1 m wide, 0.25 m long, thickness $t_1 = 0.0355 \text{ m}$, $t_2 = 0.021 \text{ m}$, $t_3 = 0.011 \text{ m}$, $t_4 = 0 \text{ m}$.

In order to form trapezoidal cross-section, different transverse slopes were settled ($I_{i1} = 0.014 \text{ m}/0.1 \text{ m} = 1/7$, $I_{i2} = 0.01 \text{ m}/0.1 \text{ m} = 1/10$, $I_{i3} = 0.011 \text{ m}/0.1 \text{ m} = 1/9$).

A point gauge with 0.1 mm reading was used to measure roughness bed surface and water surface every 25 cm interval in longitudinal horizontal direction (x-direction). The roughness bed is assessed at

transverse coordinate (y-coordinate): $y = 0.05, 0.15, 0.25, 0.35$, and 0.38 m (where $y = 0 \text{ cm}$ is the right side wall of the channel, $y = 40 \text{ cm}$ the left side wall), while the water surface for the region of total width of water flow.

The flow velocity was measured every 0.25 m interval in x-direction and y-coordinates 0.015, 0.05, 0.10, 0.15, 0.25, and 0.35 m. The used propeller current

meter (Model VR-301/VR3T-4-20N, KENEK CO., LTD) measures both longitudinal u (in x -direction) with sampling time of 20 seconds (for a total of 167 point measurements). The instrument’s sensitivity is ± 5 cm/s [6].

2.1 Characteristics of Bed Profile

Longitudinal bed profiles are shown in Fig. 1. The elevation of bed profile depends on the relative transverse coordinate y/B . In this case, the measurement point is the top of boulders (yellow marked). As the boulder is stacked on each step, 1/25 slope is settled as averaged slope. As shown in Photo 3, longitudinal slope is locally changed, and it is easy to reduce the flow velocity. The stacked boulders may help the migration of multi-aquatic animals [7-9] and also the velocity decay during flood stages.

Fig. 2 shows bed profiles on 4th step in which is counted from the upstream end of stepped channel. Here, x_{sp} is longitudinal distance from the drop of each step in proto type. Z_p is elevation for the surface of the stacked boulder in proto type. As shown in this figure, the elevation of the stacked boulder around downstream end of step is apt to be higher than that around upstream end of step. As the boulder stacked at end sill is significant, the long size of the boulder is relatively larger than that on the step. Accordingly, water depth required for the migration of multi-aquatic animals can be kept locally near the water side.

Fig. 3 shows transverse bed profiles on 4th step. As shown in this figure, averaged slope can be regarded as 1/8 slope. By considering the installation of stacked boulders on different transverse slopes (see Table 1), the shape of cross section is regarded as a parabolic shape, and the formation of diverse flow near the water side might be kept for a wide range of normal discharges (e.g., from 0.45 to 3.2 m³/s).

2.2 Characteristics of Velocity in Roughness Region

Fig. 4 shows the relationship between velocity u_p

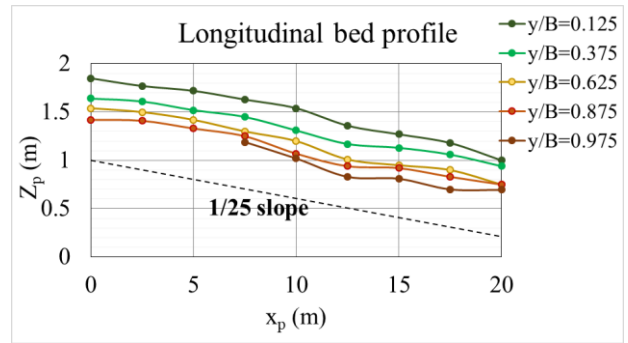


Fig. 1 Longitudinal bed profiles in roughness region.



Photo 3 Measurement points (yellow) for bed profile.

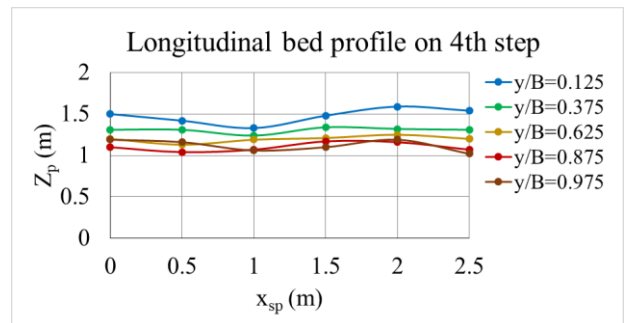


Fig. 2 Longitudinal bed profiles on 4th step.

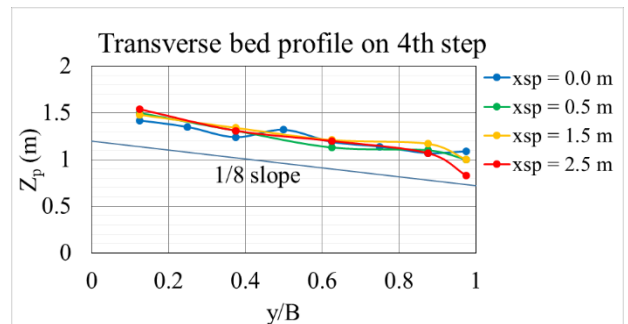


Fig. 3 Transverse bed profiles at 4th step.

and water elevation based on top of boulder d_p converted in proto type. In this figure, the data in the range of $4.4 < x_p(m) < 17.5$ were plotted by neglecting the effect of the local flow near the upstream and downstream ends of roughness region, and the data for Cases 1, 2, and 3 were utilized. Then, the flow condition in which supercritical flow is formed at the

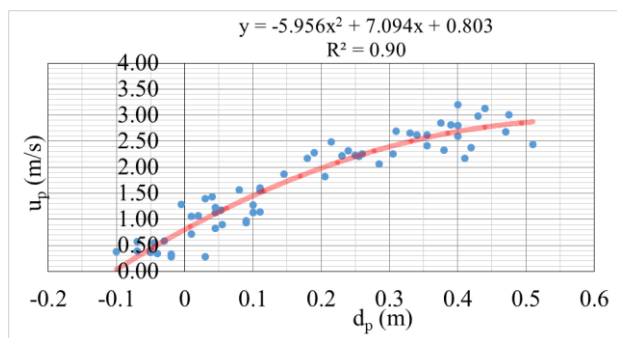


Fig. 4 Relationship between velocity and water elevation based on top of boulder.

downstream end of roughness region has been investigated. As shown in Fig. 4, the relation between the velocity on the roughness bed and the water elevation based on top of boulder might be independent of the measurement position in the range of $4.4 < x_p(\text{m}) < 17.5$, and can be predicted by the following equation.

$$u_p = -5.956 \times d_p^2 + 7.094 \times d_p + 0.803 \quad (1)$$

Autocorrelation coefficient: $R^2 = 0.90$.

If the water depth on stacked boulders is estimated in each region shown in Photo 2, the discharge per unit width can be predicted by using equation (1). For Case 4, the application of Eq. (1) might be predicted the velocity field on stacked boulders in the range of $4.4 < x_p(\text{m}) < 17.5$ without the velocity measurement. Further, if the cross section is extended as symmetric trapezoidal section, the total discharge might be calculated.

3. Results and Discussion

3.1 Description of the Flow Conditions

Flow condition depends on longitudinal slope, transverse slope, roughness region (longitudinal length and width), the size of stacked boulder, and discharge. All experiments were conducted in a rectangular channel with 17 m long, 0.6 m height, and channel width $B = 0.4$ m. These investigations were studied as a first stage, and longitudinal slope, transverse slope, roughness region (longitudinal length and width), and the size of stacked boulder were fixed.

For Case 1 ($Q_p = 0.45 \text{ m}^3/\text{s}$ in proto type), the total width of water flow occupies 62.5% of the width of

roughness region. Also, the gap flow is formed near the water side. At left side, as shown in Photo 4, around 0.2 m depth in proto type can be kept by shape resistance due to stacked boulders [10].

For Case 4 ($Q_p = 0.99 \text{ m}^3/\text{s}$ in proto type), as shown in Photo 5, the total width of water flow reaches the width of roughness region. Also, the formation of gap flow can be kept near the right side.

For Case 2 ($Q_p = 1.9 \text{ m}^3/\text{s}$ in proto type), as shown in Photo 6, the water level at right side is located at the top of boulders in a quasi-uniform flow region. The subcritical flow is formed at the right side, while the supercritical flow is formed at left side.

For Case 3 ($Q_p = 3.2 \text{ m}^3/\text{s}$ in proto type), as shown in Photo 7, the formation of supercritical and subcritical flows can be found at left side, and the flow velocity around left side can be reduced by flow resistance due to sacked boulders [10]. A gap flow among stacked boulders might be helpful for the migration of multi-aquatic animals.

For Case 5 ($Q_p = 12.2 \text{ m}^3/\text{s}$ in proto type), the supercritical flow is formed in the roughness region. If the tailwater level is larger than 1.56 m above the



Photo 4 Flow condition for Case 1 (left side view).



$Q_p = 0.451 \text{ m}^3/\text{s}$ for Case 1
 $Q_p = 0.986 \text{ m}^3/\text{s}$ for Case 4

Photo 5 Flow condition for Case 4 (Bird view).



Photo 6 Flow condition for Case 2 (Right side view).



Photo 7 Flow condition for Case 3 (Right side view).

bottom at downstream end, the main flow passing over the roughness region is located near the water surface. The installation of stacked boulders has been stable.

3.2 Bed and Water Surface Profiles

The data of water surface for Case 1 were collected at $y/B = 0.625, 0.875, \text{ and } 0.975$.

Fig. 5 shows bed and water surface profiles for Case 1 ($Q_p = 0.455 \text{ m}^3/\text{s}$). Then, the data for $y/B = 0.975$ were measured in the range of $7.5 < x_p(\text{m}) < 20$. When the supercritical flow is formed in the roughness region, the transition from supercritical to subcritical flows is formed at the downstream of the roughness region, and a surface jet flow is formed. As shown in Fig. 5, the water surface profile changes smoothly around $x_p = 20 \text{ m}$.

Figs. 6 and 7 show transverse bed and water surface profiles at $x_p = 10 \text{ m}$ and 15 m , respectively. The water surface profile is shown in the region $3.0 < y_p(\text{m}) < 4.0$. Also, the transverse slope of water surface goes up to the left. In this case, a gap flow is formed in stacked boulders, and flooding region is extended to $y_p = 1.5 \text{ m}$. As the bed profile is shown by connecting with the measurement point around top of boulder, the water flow depth might be underestimated. It is possible for swimming fishes to keep the migration route, even if the discharge reaches to $0.452 \text{ m}^3/\text{s}$ as a lower limit. Crustacean and benthic fish might migrate upstream easily in gap flow region.

The data of water surface for Case 4 were collected at $y/B = 0.125, 0.375, 0.625, 0.875, \text{ and } 0.975$.

Fig. 8 shows bed and water surface profiles for Case 4 ($Q_p = 0.986 \text{ m}^3/\text{s}$). Then, the data for $y/B = 0.975$ were measured in the range of $7.5 < x_p(\text{m}) < 20$. In

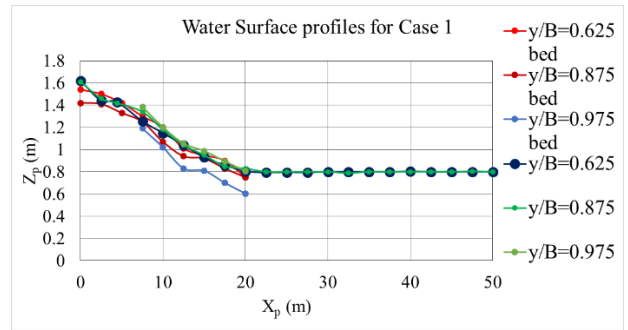


Fig. 5 Bed and Water Surface profiles for Case 1.

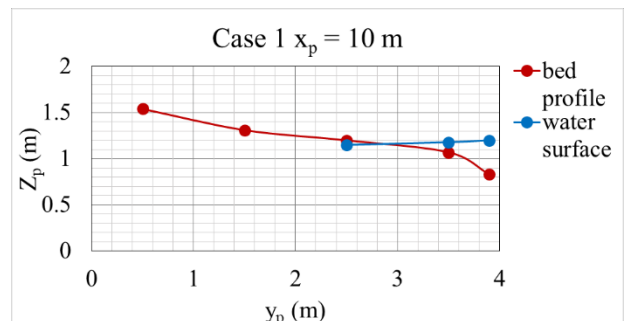


Fig. 6 Transverse water surface profile at $x_p = 10 \text{ m}$.

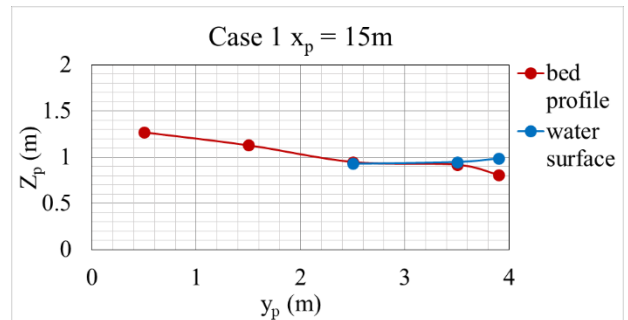


Fig. 7 Transverse water surface profile at $x_p = 15 \text{ m}$

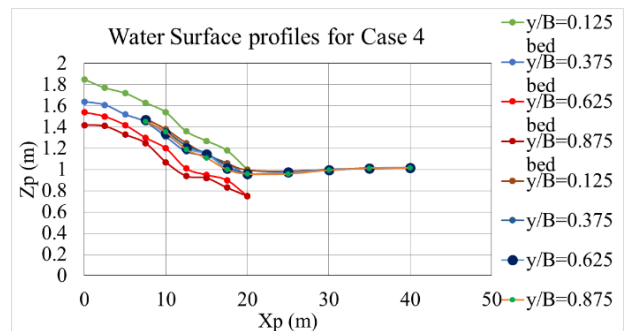


Fig. 8 Bed and water surface profiles for Case 4.

the transition from supercritical to subcritical flow at the downstream of $x_p = 20 \text{ m}$, as a surface jet flow is formed, the water surface profile changes smoothly. Also, the water surface level increases gradually in the

range of $20 < x_p(m) < 40$, because the momentum flux passing over the stacked boulder is large.

Figs. 9 and 10 show transverse bed and water surface profiles at $x_p = 10$ m and 15 m, respectively. The water surface profile is shown in the region $1.5 < y_p(m) < 4.0$. In this case, the formation of a gap flow can be found until the right side $y_p = 0$ m. The transverse slope of water surface is almost flat in the region $0 < y_p(m) < 4.0$.

The data of water surface for Case 2 were collected at $y/B = 0.125, 0.375, 0.625,$ and 0.875 .

Fig. 11 shows bed and water surface profiles for Case 2 ($Q_p = 1.88 \text{ m}^3/\text{s}$). As in the case of Cases 1 and 4, as a surface jet flow is formed, the water surface profile changes smoothly around $x_p = 20$ m. Also, the water surface level increases gradually in the range of $20 < x_p(m) < 40$.

Fig. 12 shows transverse bed and water surface profiles at $x_p = 10$ m. The water surface profile is shown in the region $0.5 < y_p(m) < 4.0$. In this case, a gap flow is formed in stacked boulders, and flooding region is extended to $y_p = 0$ m. Also, the transverse slope of water surface is almost flat in the region $2.5 < y_p(m) < 4.0$.

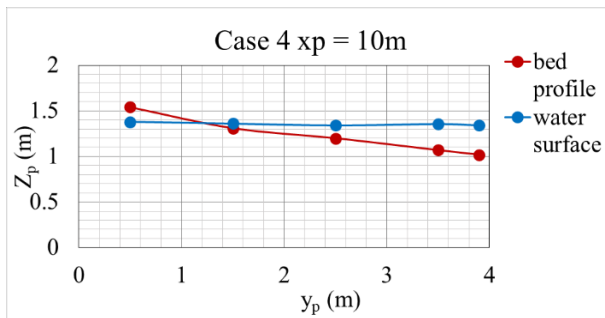


Fig. 9 Transverse water surface profile at $x_p = 10$ m.

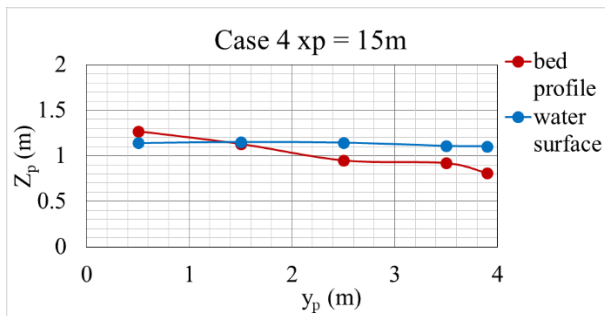


Fig. 10 Transverse water surface profile at $x_p = 15$ m.

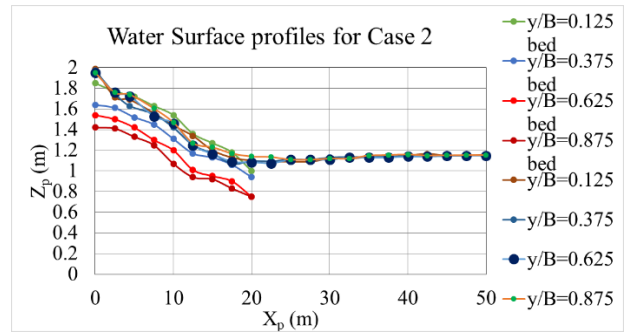


Fig. 11 Bed and water surface profiles for Case 2.

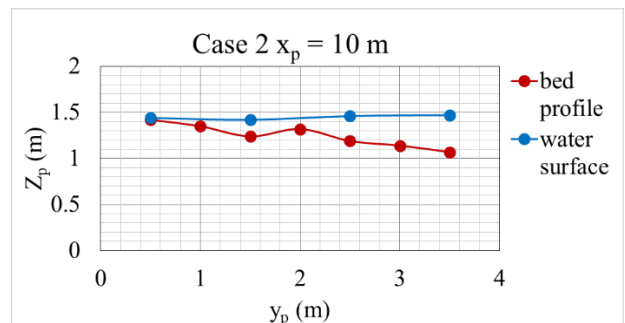


Fig. 12 Transverse water surface profile at $x_p = 10$ m.

Fig. 13 shows bed and water surface profiles for Case 3 ($Q_p = 3.25 \text{ m}^3/\text{s}$). As the discharge is increased, the water surface level increases gradually in the range of $20 < x_p(m) < 50$.

Figs. 14 and 15 show transverse bed and water surface profiles at $x_p = 10$ m and 15 m, respectively. The water surface profile is shown in the region $0 < y_p(m) < 4.0$. In this case, the transverse slope of water surface goes up to the left in the region $0 < y_p(m) < 2.5$. A different water surface profile can be found between $x_p = 10$ m and 15 m, because an undular surface is formed on the stacked boulder (see Fig. 13).

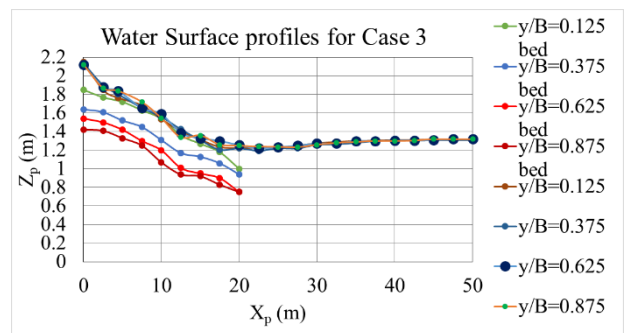


Fig. 13 Bed and water surface profiles for Case 3.

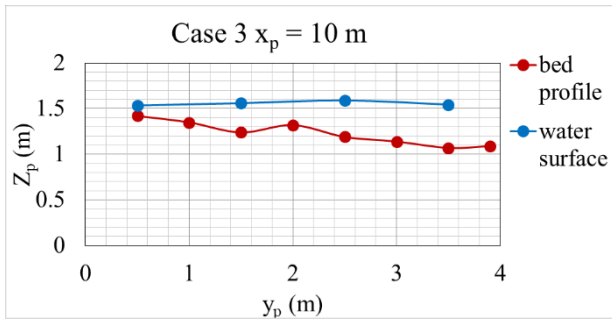


Fig. 14 Transverse water surface profile at $x_p = 10$ m.

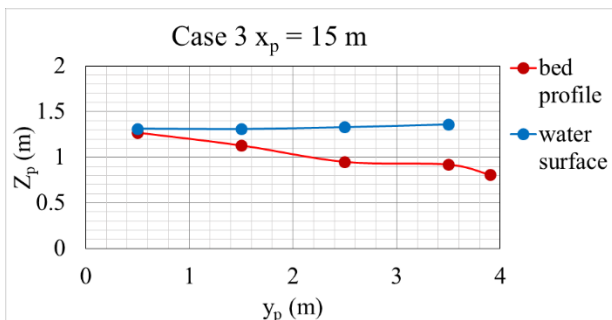


Fig. 15 Transverse water surface profile at $x_p = 15$ m.

Accordingly, if the discharge is changed from 0.455 m^3/s to 3.25 m^3/s , a shallow flow is always formed near the water side. At the location of $y/B = 0.975$ for Case 1, as shown in Figs. 16 and 17, the water flow depth on the stacked boulder is varied in the range of $0.06 < d_p(m) < 0.28$. Then, it should be noted that the water depth shown in Fig. 17 is evaluated as a depth on the stacked boulder. The roughness mild slope with stacked boulders can keep the migration route under a wide range of discharges.

3.3 Velocity Fields

In order to find the possibility of upstream migration for different discharges, velocity fields on the stacked boulder are shown in Figs. 18-21. For Case 4, as the

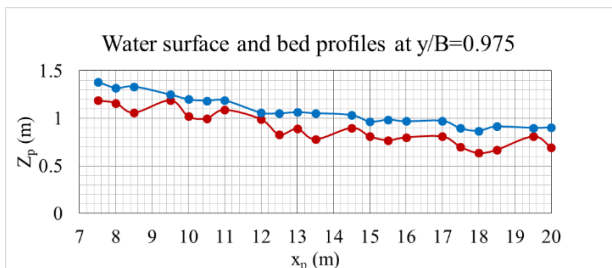


Fig. 16 Bed and water surface profiles at $y/B = 0.975$ (Case 1).

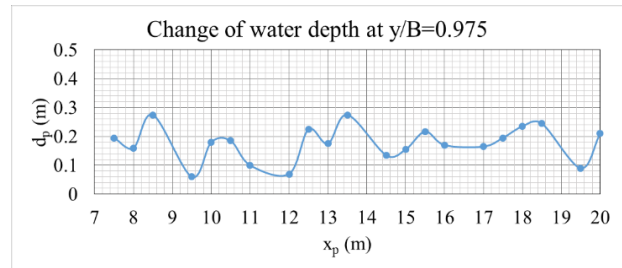


Fig. 17 Change of water depth at $y/B = 0.975$ (Case 1).

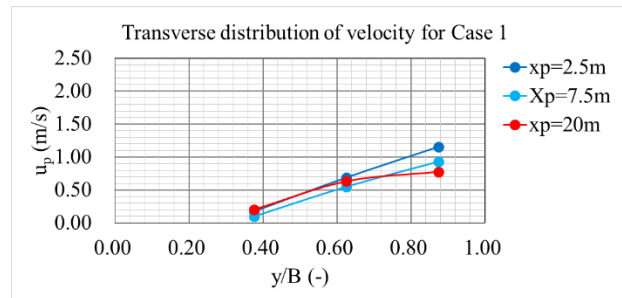


Fig. 18 Transverse distribution of velocity for Case 1.

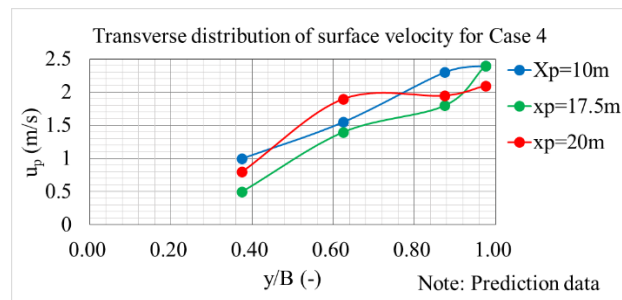


Fig. 19 Transverse distribution of velocity for Case 4.

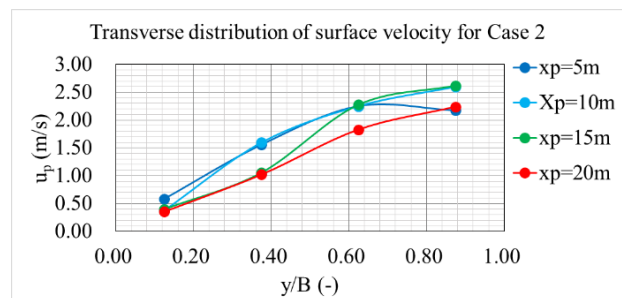


Fig. 20 Transverse distribution of velocity for Case 2.

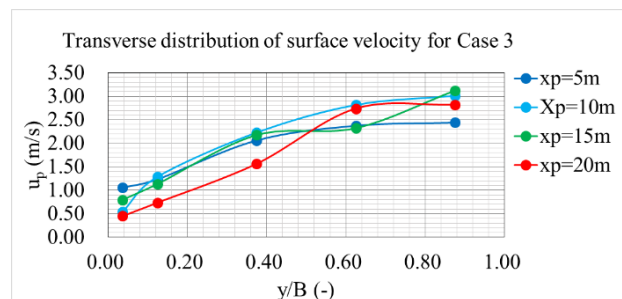


Fig. 21 Transverse distribution of velocity for Case 3.

water flow depth was measured, the velocity on the stacked boulder could be predicted by using Eq. (1).

For Case 1, the velocity changes with transverse coordinate y/B , and the velocity in the range of $0.375 < y/B < 1.0$ might enable the upstream migration for multi-aquatic animals (Fig. 18).

For Case 4, the velocity in the range of $y/B < 0.6$ might enable the upstream migration, because the velocity u_p is reduced to 1.5 m/s (Fig. 19).

For Cases 2 and 3, as the discharge is increased, the velocity on the stacked boulder becomes larger. Also, as the total width of water flow reaches to the channel width, the velocity field for $u_p < 1.5$ m/s is limited (Figs. 20 and 21). At the downstream of $x_p = 20$ m, the velocity field is affected the transition from supercritical to subcritical flows.

The velocity field downstream of the stacked boulder is important for leading multi-aquatic animals to the migration route. For Case 1, the surface velocity decays in a short distance (Fig. 22), even if the main flow is located near the water surface. While, for Cases 2 and 3, the surface velocity with $u_p > 1$ m/s is continued in the region of $20 < x_p(m) < 40$ (Figs. 23 and 24). For Case 4, a similar velocity field might be expected from the predicted velocity field on the stacked boulder (Fig. 19).

Figs. 25-27 show longitudinal change of surface velocity for Cases 1, 2, and 3.

The velocity is accelerated on the roughness bed with stacked boulder, and the maximum velocity occurs on the roughness region at $y/B = 0.875$ (Cases 1, 2, and 3), 0.625, and 0.375 (Cases 2 and 3). The

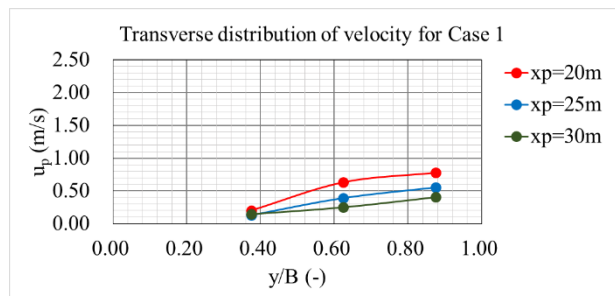


Fig. 22 Transverse distribution of velocity below the stacked boulder for Case 1.

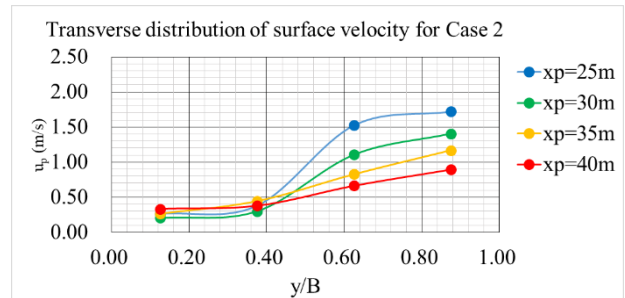


Fig. 23 Transverse distribution of velocity below the stacked boulder for Case 2.

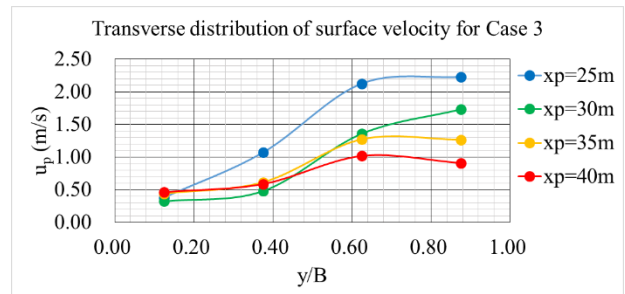


Fig. 24 Transverse distribution of velocity below the stacked boulder for Case 3.

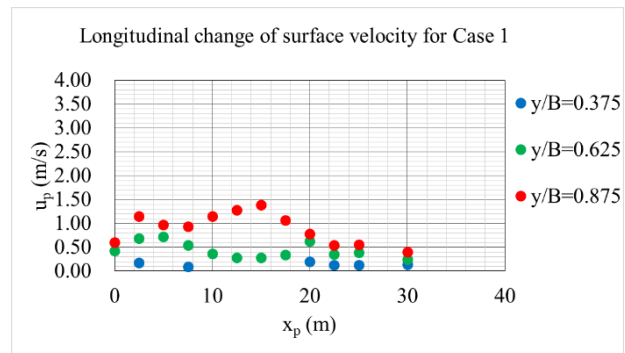


Fig. 25 Longitudinal change of surface velocity for Case 1.

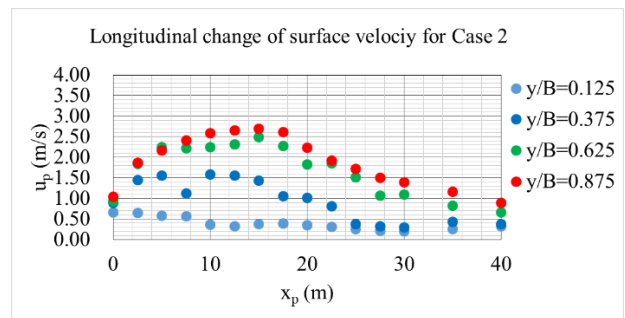


Fig. 26 Longitudinal change of surface velocity for Case 2.

maximum position does not reach the downstream end of stacked boulder. If the length of roughness bed with stacked boulders is longer, a quasi-uniform flow is formed on the way of the roughness bed, and the

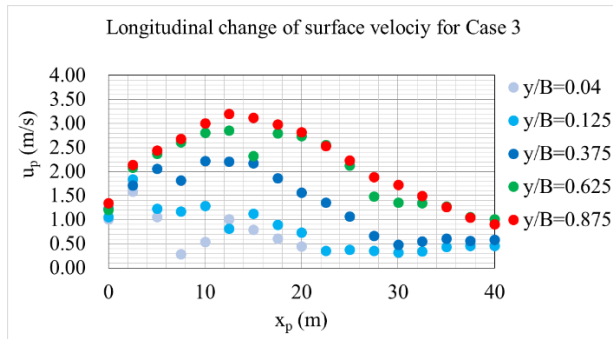


Fig. 27 Longitudinal change of surface velocity for Case 3.

acceleration region might not be extended. Regarding the surface velocity decay downstream of the sacked boulder, the surface velocity with $u_p > 1$ m/s is continued in the region of $20 < x_p$ (m) < 40 for Cases 2 and 3 (Figs. 23, 24, 26, and 27). While, for Case 1, the surface velocity is reduced within $0.4 < u_p$ (m/s) < 0.8 , and the main flow passing over the roughness bed might not be helpful as a guide flow which leads swimming and benthic fishes.

By considering the surface velocity downstream of the fish passage and the velocity on the stacked boulder for the upstream migration, the discharge should be controlled in the range of $0.9 < Q_p$ (m³/s) < 3.3 , and the function as a fish passage might be kept.

4. Conclusion

The roughness mild slope with stacked boulders was proposed as a new fish passage by considering guide flow and migration route under a wide range of discharges. The roughness bed is consisted by the stacked boulders with around 0.5 m long size. In order to install the stacked boulder in the area with 1.0 m wide and 2.5 m long, the stepped channel with 0.1 m drop is installed on longitudinal slope 1/25 and transverse slope around 1/8. Also, the vertical sill with 0.2 m height is installed at upstream end of each step for the first installation of stacked boulder on the step.

Flow characteristics on the stacked boulder were investigated experimentally on the basis of Froude similarity. The physical scale was settled as 1/10 scale by considering the installation of physical model in a rectangular channel with 17 m long, 0.4 m wide, and

0.6 m height. As the stacked boulders with around 0.5 m long size is utilized in proto-type, it is possible to form seepage flow near the water side, and the combination between gap flow and shallow water flow enables upstream migration for multi-aquatic animals. The relationship between bed and water surface profiles yields that gap and shallow water flows are formed in the range of $0.42 < Q_p$ (m³/s) < 3.3 .

The relation between the velocity on the roughness bed and the water elevation based on top of boulder might be independent of the measurement position in the range of $4.4 < x_p$ (m) < 17.5 . If the water depth on stacked boulders is estimated in each region, the discharge per unit width can be predicted. Further, if the cross section is extended as symmetric trapezoidal section, the total discharge might be calculated.

Velocity fields on the stacked boulder yield the possibility of upstream migration in the range of $0.42 < Q_p$ (m³/s) < 3.3 . Also, if the discharge is in the range of $0.98 < Q_p$ (m³/s) < 3.3 , the surface velocity with $u_p > 1$ m/s may help to lead multi-aquatic animals the downstream end of the stacked boulder. Regarding the surface velocity decay downstream of the sacked boulder, the surface velocity with $u_p > 1$ m/s is continued in the region of $20 < x_p$ (m) < 40 for Cases 2 and 3 ($Q_p = 1.88$ and 3.25 m³/s).

Accordingly, if the fish passage with 4 m wide is installed as the roughness mild slope (1/25 slope) with the stacked boulder (around 0.5 m size), the discharge in the range of $0.9 < Q_p$ (m³/s) < 3.3 may help the upstream migration of multi-aquatic animals.

References

- [1] Y. Yasuda, Guideline of Fish passage — For engineers, Hokkaido Fishway Society edit, Corona Company, 2011, p. 141, available online at: <http://www.coronasha.co.jp/np/isbn/9784339052336/>. (in Japanese)
- [2] Y. Yasuda, *Contribution Due to River Engineering in Preservation for Diadromous Aquatic Animals*, No. 225, Vol. 38, No. 4, Aqua-biology, Seibutsu Kennkyusha Co. Ltb. 2016, pp. 387-396. (in Japanese)
- [3] Y. Yasuda and Y. Seo, What should civil engineers learn from failures in fishways? In: *33rd IAHR Congress, Water Engineering for a Sustainable Environment*, IAHR,

- Vancouver, Canada, CD-ROM, 2009.
- [4] Y. Yasuda, New fishway design for slit-type Sabo dams and effect of the fishway on migration of aquatic animals, in: A. A. Balkema, *Fluvial Environmental and Coastal Developments in Hydraulic Engineering*, Taylor & Francis Group, London, 2004, pp. 115-131.
- [5] Y. Yasuda and T. Ohnishi, Relationship between migration route of swimming fishes and velocity characteristics in pool-type fishways with a trapezoidal section, in: *33rd IAHR Congress: Water Engineering for a Sustainable Environment*, IAHR, Vancouver, Canada, CD-ROM, 2009.
- [6] KENEK CO., LDT, propeller Current Meter: Detector MODEL: VR-301/VR3T-3-20N VR3T-4-20N. VR3T-2-20K VR3T-3-20K VR3T-4-20K, product information sheet, Tokyo, Japan, accessed on 2021.09.06, available online at: [https://www.sokken.com](https://www.sokken.com/img/120406094031.pdf)
- [7] Y. Yasuda and M. Uchimura, Fish passage based on stone masonry with stacking boulders, in: *International Symposium of Ecohydraulics*, Tokyo, Japan, SS38, CD-ROM, 2018.
- [8] Y. Yasuda, Improvement of flow condition in channelized river due to stacked boulders, IOP Conf. Series: Earth and Environmental Science 626, 012001, ACEER 2020, doi: 10.1088/1755-1315/626/1/012001, 2021.
- [9] Y. Yasuda, Practical approach from experimental investigation on fish passage with stacking boulders installed in weir, *Advances in River Engineering* 24 (2018) 125-130. (in Japanese)
- [10] R. D. Hey, Flow resistance in gravel-bed rivers, *Journal of Hydraulic Division* 91 (1979) (4) 365-379.